RESEARCH ARTICLE

A Melanoma Cell State Distinction Influences Sensitivity to MAPK Pathway Inhibitors

David J. Konieczkowski[1,2], Cory M. Johannessen[1,2], Omar Abudayyeh[1], Jong Wook Kim[1,2], Zachary A. Cooper[7,8], Adriano Piris[3], Dennie T. Frederick[4], Michal Barzily-Rokni[1], Ravid Straussman[1], Rizwan Haq[5,6], David E. Fisher[5,6], Jill P. Mesirov[1], William C. Hahn[1,2], Keith T. Flaherty[5], Jennifer A. Wargo[7,8], Pablo Tamayo[1], and Levi A. Garraway[1,2]

ABSTRACT Most melanomas harbor oncogenic $BRAF^{V600}$ mutations, which constitutively activate the MAPK pathway. Although MAPK pathway inhibitors show clinical benefit in $BRAF^{V600}$-mutant melanoma, it remains incompletely understood why 10% to 20% of patients fail to respond. Here, we show that RAF inhibitor–sensitive and inhibitor-resistant $BRAF^{V600}$-mutant melanomas display distinct transcriptional profiles. Whereas most drug-sensitive cell lines and patient biopsies showed high expression and activity of the melanocytic lineage transcription factor MITF, intrinsically resistant cell lines and biopsies displayed low MITF expression but higher levels of NF-κB signaling and the receptor tyrosine kinase AXL. *In vitro*, these MITF-low/NF-κB–high melanomas were resistant to inhibition of RAF and MEK, singly or in combination, and ERK. Moreover, in cell lines, NF-κB activation antagonized MITF expression and induced both resistance marker genes and drug resistance. Thus, distinct cell states characterized by MITF or NF-κB activity may influence intrinsic resistance to MAPK pathway inhibitors in $BRAF^{V600}$-mutant melanoma.

SIGNIFICANCE: Although most $BRAF^{V600}$-mutant melanomas are sensitive to RAF and/or MEK inhibitors, a subset fails to respond to such treatment. This study characterizes a transcriptional cell state distinction linked to MITF and NF-κB that may modulate intrinsic sensitivity of melanomas to MAPK pathway inhibitors. *Cancer Discov; 4(7); 816–27. ©2014 AACR.*

INTRODUCTION

Mutations affecting codon 600 of the serine/threonine kinase BRAF are among the most highly recurrent genetic aberrations in melanoma (1, 2). These mutations activate the downstream kinases MEK and ERK within the MAPK pathway, leading to enhanced cellular proliferation and survival. The discovery that $BRAF^{V600}$ mutations predict sensitivity to MAPK pathway inhibitors (3) revolutionized therapeutic approaches to melanoma. MAPK pathway inhibitors—including the RAF inhibitors (RAFi) vemurafenib and dabrafenib and the MEK inhibitor (MEKi) trametinib—achieve clinical benefit in 80% to 90% of patients with $BRAF^{V600}$-mutant melanoma (4–6). However, among patients whose tumors respond to MAPK pathway inhibitors, relapse is universal (acquired resistance). Moreover, 10% to 20% of patients never achieve meaningful response to therapy (innate or intrinsic resistance).

Recent studies have characterized numerous mechanisms of acquired resistance to MAPK pathway inhibitors in $BRAF^{V600}$-mutant melanoma. These include activating mutations in the downstream kinase MEK (7–9) as well as acquisition of an inhibitor-resistant *BRAF* splice variant (10). Alternative MAP3K proteins [e.g., CRAF (11) or COT (12)] are also able to reengage the MAPK pathway in the presence of BRAF inhibition. Similarly, upstream of RAF proteins, activation of RAS signaling [e.g., by mutation (13), NF1 loss (14, 15), or relief of negative feedback (16)] confers RAFi resistance. Cumulatively, these studies have most commonly converged upon reactivation of the MAPK pathway as a common effector of many mechanisms of acquired resistance.

In contrast, fewer studies have directly queried intrinsic resistance to RAF inhibition in melanoma. Two recent studies examined stromal contributions to intrinsic resistance. This work identified stromal secretion of hepatocyte growth factor (HGF), activation of the receptor tyrosine kinase MET, and subsequent MAPK pathway reactivation as a mechanism of intrinsic MAPK pathway inhibitor resistance in melanoma (17, 18). It remains largely unknown, however, whether cell-autonomous differences might also contribute to the intrinsic resistance phenotype. Therefore, we sought to elucidate molecular features that might mediate intrinsic resistance to RAF/MEK inhibition in $BRAF^{V600}$-mutant melanoma.

RESULTS

We hypothesized that cell-autonomous differences, such as distinct gene expression programs, might partially account for why some melanomas display intrinsic resistance to MAPK pathway inhibitors. To test this hypothesis, we examined 29 $BRAF^{V600}$-mutant melanoma cell lines from the Cancer Cell Line Encyclopedia (CCLE; ref. 19) for which gene expression and pharmacologic sensitivity data were available (Fig. 1A). Although most lines were sensitive to the RAFi PLX4720 ($GI_{50} \leq 2$ μmol/L), some exhibited intrinsic resistance to this agent ($GI_{50} = 8$ μmol/L, the maximum of this assay; Fig. 1A) as well as to MEKi (PD0325901 and AZD6244; Fig. 1B). To assess

Authors' Affiliations: [1]Broad Institute of Harvard and MIT, Cambridge; [2]Department of Medical Oncology, Dana-Farber Cancer Institute; Divisions of [3]Dermatopathology and [4]Surgical Oncology, [5]Massachusetts General Hospital Cancer Center, and [6]Dermatology and Cutaneous Biology Research Center, Massachusetts General Hospital, Boston, Massachusetts; Departments of [7]Surgical Oncology, and [8]Genomic Medicine, The University of Texas MD Anderson Cancer Center, Houston, Texas

Note: Supplementary data for this article are available at Cancer Discovery Online (http://cancerdiscovery.aacrjournals.org/).

D.J. Konieczkowski and C.M. Johannessen contributed equally to this work.

Corresponding Author: Levi A. Garraway, Department of Medical Oncology, Dana-Farber Cancer Institute, 450 Brookline Avenue, Boston, MA 02215. Phone: 617-632-6689; Fax: 617-582-7880; E-mail: levi_garraway@dfci.harvard.edu

doi: 10.1158/2159-8290.CD-13-0424

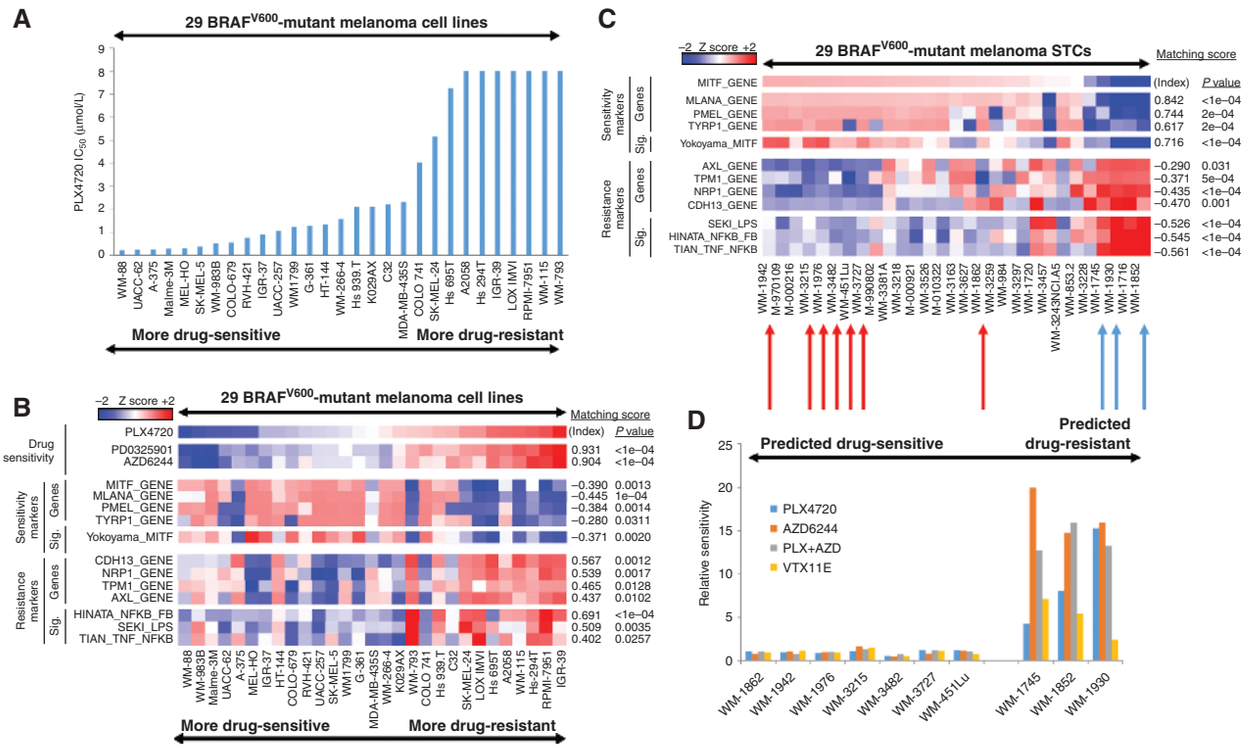

Figure 1. Association of expression classes with differential MAPK pathway inhibitor sensitivity in BRAF^{V600}-mutant melanoma *in vitro*. **A,** sensitivity to PLX4720 (RAFi) across a collection of BRAF^{V600}-mutant melanoma cell lines. **B,** relationship between PLX4720 sensitivity and MITF-high versus NF-κB–high classes. **C,** transcriptional class distinction in BRAF^{V600}-mutant melanoma short-term cultures (STC). Red arrows identify cell lines predicted to be drug sensitive; blue arrows identify cell lines predicted to be drug resistant. **D,** relationship in short-term cultures between expression class and MAPK pathway inhibitor sensitivity. Graph shows GI_{50} values relative to median GI_{50} of the sensitive short-term cultures. PLX4720, RAFi; AZD6244, MEKi; VTX11E, ERK inhibitor (ERKi).

whether differences in transcriptional programs existed between intrinsically sensitive and resistant lines, we identified genes whose expression across the cell lines was strongly correlated or anticorrelated with their PLX4720 GI_{50} values. *MITF*, which encodes a melanocyte lineage regulatory transcription factor and melanoma oncogene (20), emerged as the single gene best correlated with sensitivity to PLX4720 (Supplementary Fig. S1A and Supplementary Table S1). Although *MITF* was strongly expressed in the majority of drug-sensitive lines, it was poorly expressed in the resistant lines (Fig. 1B and Supplementary Fig. S2). Because MITF transcriptional activity can be regulated separately from MITF expression levels, we also measured MITF function by querying expression of MITF target genes *PMEL*, *TYRP1*, and *MLANA*, as well as a global transcriptional signature of MITF activity (21). These too were poorly expressed in the resistant lines, implying a reduction not only in expression but also in activity of MITF (Fig. 1B, Supplementary Fig. S2, and Supplementary Table S1). Instead, drug-resistant BRAF^{V600}-mutant melanoma cell lines displayed multiple expression signatures of NF-κB activation, suggesting elevated NF-κB transcriptional activity (Fig. 1B). Correspondingly, levels of phosphorylated, activated RELA (an NF-κB transcription factor; ref. 22) were increased in the majority of resistant lines relative to the sensitive lines (Supplementary Fig. S2). Resistant lines also expressed individual marker genes such as *AXL*, *TPM1*, *NRP1*, and *CDH13* (Fig. 1B and Supplementary Fig. S2) that were not observed in the sensitive lines. These genes have not been previously characterized as MITF- or NF-κB–associated, but they nominated additional features that might be associated with the MITF-low/NF-κB–high transcriptional state.

Because prosurvival signaling through NF-κB has previously been associated with resistance to cytotoxic therapies, such as doxorubicin (23), we sought to assess whether the NF-κB–high state was associated with generalized drug resistance. However, among 24 targeted and cytotoxic anticancer drugs, differential MITF expression levels were strongly correlated with differential sensitivity only to the four MAPK inhibitors (MAPKi) tested (Supplementary Fig. S3). This finding suggests that the MITF-low/NF-κB–high transcriptional state may pertain specifically to resistance to MAPK pathway inhibition.

To verify that the MITF/NF-κB class distinction was reproducibly associated with differential sensitivity to MAPK pathway inhibition, we examined a collection of patient-derived BRAF^{V600}-mutant melanoma short-term cultures for which gene expression data, but not pharmacologic sensitivity data, were available. As in other datasets, we identified reciprocity between MITF and NF-κB levels across this collection (Fig. 1C and Supplementary Fig. S4). This relationship was evident for MITF itself as well as for both the MITF transcriptional signature as a whole (Fig. 1C) and individual MITF target genes (Fig. 1C and Supplementary Fig. S4), confirming that MITF transcriptional activity varied together with MITF expression across these

samples. Correspondingly, both NF-κB–related gene expression levels (e.g., AXL; Fig. 1C and Supplementary Fig. S4) and transcriptional signatures of NF-κB pathway activity (Fig. 1C) varied across the collection in a manner similar to that of the initial melanoma cell line panel. Similarly, phosphorylated, activated levels of the NF-κB transcription factor RELA (Supplementary Fig. S4) also segregated inversely with MITF activity.

Next, we performed pharmacologic growth inhibition studies on seven MITF-high and three NF-κB–high short-term cultures. As predicted, all seven MITF-high/NF-κB–low short-term cultures were sensitive to RAF and MEK inhibition, whereas each of the three MITF-low/NF-κB–high short-term cultures was resistant to these agents (Fig. 1D). These findings supported the premise that the MITF-low/NF-κB–high transcriptional signature correlated with resistance to MAPK pathway inhibition in $BRAF^{V600}$-mutant melanoma.

We next sought to assess whether this intrinsic resistance phenotype might derive from incomplete MAPK pathway inhibition, as opposed to indifference to MAPK pathway inhibition in these cells. First, we noted that MITF-low/NF-κB–high short-term cultures (Fig. 1D) and cell lines (Supplementary Fig. S5) showed resistance not only to single-agent RAF and MEK inhibition, but also to combined RAF–MEK inhibition and ERK inhibition (VTX11E), suggesting that intrinsic resistance extends to multiple levels of the RAF–MEK–ERK signaling cascade. Moreover, the resistance phenotype was not clearly attributable to incomplete MAPK pathway suppression by these agents, because the reduction of phosphorylation of both ERK and the ERK substrate FRA1 in resistant lines following exposure to RAFi, MEKi, and ERK inhibitors (ERKi) was comparable with that observed in sensitive lines (Supplementary Fig. S6). Unique among the tested resistant lines, RPMI-7951 cells maintain MAPK pathway activity even in the setting of inhibitor treatment (Supplementary Fig. S6); however, this line also harbors amplification of *MAP3K8*/*COT*, which is sufficient to reactivate ERK signaling following inhibition of RAF and/or MEK in this cell line (12).

Consistent with prior literature (24, 25), the ERKi VTX11E did not inhibit phosphorylation of ERK itself. Nonetheless, the magnitude of phosphorylated FRA1 (pFRA1) suppression by VTX11E was comparable with that induced by the ERKi SCH772984 (25), which inhibits both ERK activity and ERK phosphorylation (Supplementary Fig. S7A). VTX11E and SCH772984 also showed a similar spectrum of sensitivity across a panel of $BRAF^{V600}$-mutant melanoma cell lines (Supplementary Figs. S4A and S7B).

In addition to showing comparable biochemical responses to MAPK pathway inhibition, sensitive and resistant short-term cultures (Supplementary Fig. S8) and cell lines (Supplementary Fig. S9) displayed no clear differences in basal phosphorylation levels of ERK or FRA1 or cell lines, implying that differential basal MAPK pathway activity does not account for differential response to MAPK pathway inhibitors. Together, these findings suggest that a molecularly defined subset of MITF-low/NF-κB–high $BRAF^{V600}$-mutant melanomas may exhibit indifference to MAPK pathway inhibition.

To confirm that the apparent reciprocity between MITF and NF-κB expression signatures was also evident *in vivo*, we examined a collection of primary and metastatic $BRAF^{V600}$-mutant melanomas from The Cancer Genome Atlas (https://tcga-data.nci.nih.gov/tcga/). In this dataset, we also observed anticorrelation between expression of *MITF* (and its activity, as measured by target genes and signature) and NF-κB activation (as measured by single-gene markers as well as an expression signature of NF-κB activity; Fig. 2A). Thus, the transcriptional class distinction that segregated MAPK pathway inhibitor–sensitive and –resistant cell lines was also discernible in melanoma tumors.

This reciprocity between MITF and NF-κB transcriptional profiles was reminiscent of prior transcriptional (26) and histopathologic (27) evidence for a two-class distinction in melanoma. These distinct gene expression programs, however, have not previously been linked to resistance to vemurafenib or dabrafenib/trametinib in $BRAF^{V600}$-mutant melanomas. Extending these prior results, our findings suggest that this transcriptional class distinction may have a previously unrecognized association with differential susceptibility to MAPK pathway inhibition.

To assess whether the resistance phenotype linked to this class distinction *in vitro* was also evident in melanoma tumors, we examined biopsy specimens from patients with metastatic $BRAF^{V600}$-mutant melanoma. Samples were obtained before treatment with MAPK pathway inhibitors; after biopsy, patients received combined RAFi–MEKi therapy. Using AXL expression as a readout of the NF-κB–high cellular state (Figs. 1B and C and 2A and Supplementary Figs. S2 and S4), we stratified the cohort into MITF-high/NF-κB–low ($n = 4$) and MITF-low/NF-κB–high ($n = 8$) groups on the basis of immunohistochemistry (Fig. 2B and Supplementary Table S2). Immunocytochemistry on known MITF-positive and AXL-positive cell lines confirmed the sensitivity and specificity of this method (Supplementary Fig. S10). Progression-free survival following dabrafenib/trametinib therapy was significantly shorter in the MITF-low/NF-κB–high group relative to the MITF-high/NF-κB–low group (median 5.0 months vs. 14.5 months; $P = 0.0313$, two-tailed t test; Fig. 2C). This finding is consistent with a possible therapeutic relevance of this two-class distinction in melanoma.

Among the individual features reproducibly associated with the resistance state was the expression of the AXL receptor tyrosine kinase. AXL has been previously identified as a mediator of acquired resistance to PLX4720 in $BRAF^{V600}$-mutant melanoma (12) and to lapatinib in EGFR-mutant lung cancer (28). Therefore, we queried whether the intrinsic resistance phenotype in some $BRAF^{V600}$-mutant melanomas might simply result from AXL expression in those lines. First, we confirmed that AXL overexpression was sufficient to confer resistance to RAFi or MEKi, singly or in combination, in three $BRAF^{V600}$-mutant, MAPK pathway inhibitor–sensitive melanoma cell lines (Fig. 3A). However, ectopic AXL expression did not consistently confer robust resistance to ERK inhibition (Fig. 3A). AXL overexpression induced AKT phosphorylation and conferred sustained ERK phosphorylation in the setting of RAF/MEK inhibition (Fig. 3B). Moreover, the level of ERK phosphorylation produced by AXL overexpression was comparable with that observed following overexpression of the known RAFi resistance effector *RAF1* (Fig. 3B; ref. 11). Consistent with prior findings, these results indicated that overexpression of AXL was sufficient to confer acquired resistance to RAFi and MEKi.

We next wished to determine whether endogenous AXL was necessary for maintenance of intrinsic resistance in the NF-κB–high $BRAF^{V600}$-mutant melanoma cells. To test this

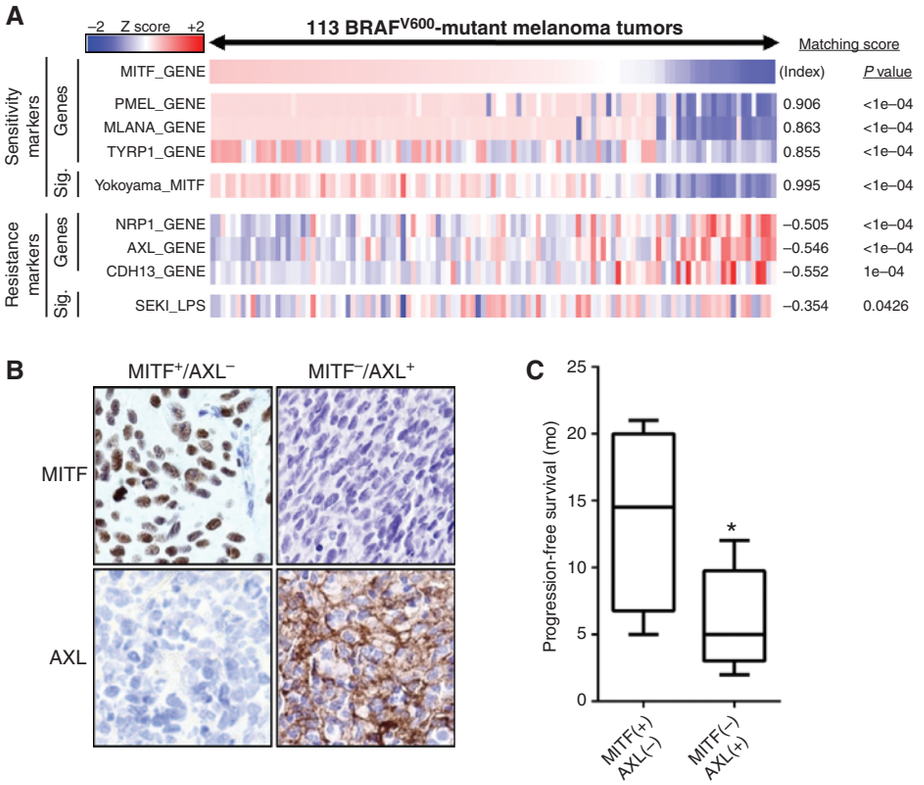

Figure 2. MITF-low/NF-κB–high transcriptional class is present and associated with resistance to MAPK pathway inhibition in human tumors. **A,** transcriptional class distinction in BRAF^{V600}-mutant melanoma tumor samples. **B,** examples of AXL and MITF staining in pretreatment melanoma biopsies (magnification, ×40). **C,** comparison of progression-free survival between MITF-positive/AXL-negative and MITF-negative/AXL-positive classes. *, $P = 0.0313$, two-tailed *t* test.

hypothesis, we used three small-molecule AXL inhibitors [R428 (29), XL184 (30), and XL880 (28, 31)]. To confirm the pharmacologic effects of these compounds, we exposed A-375 melanoma cells engineered to overexpress AXL to each drug *in vitro*. All three compounds abrogated AXL-mediated induction of AKT phosphorylation and rescue of ERK phosphorylation (Fig. 3C) but had no effect on pAKT or pERK levels in A-375 or other sensitive cell lines in the absence of exogenous AXL expression (Supplementary Fig. S11).

Next, we assessed the effects of these small molecules on intrinsically resistant melanoma cell lines that express endogenous AXL. In contrast to the setting of ectopic AXL expression, we observed no effect of the AXL inhibitors on pAKT or pERK levels in the intrinsically resistant lines, either at baseline or following treatment with PLX4720 (Fig. 3D). (AXL inhibitors also did not alter pERK or pAKT levels in intrinsically sensitive lines; Supplementary Fig. S11.) Similarly, treatment with AXL inhibitors did not alter the PLX4720 GI_{50} values of any of the intrinsically resistant melanoma lines (Fig. 3E). Comparable results were observed following knockdown of *AXL* using three independent shRNAs (the most effective of nine tested; Supplementary Figs. S12 and S13). Here, we noted that a single *AXL* shRNA (575) modulated PLX4720 GI_{50} values; although this finding could be due to marginally more effective knockdown with this shRNA, the failure of the other *AXL* shRNAs and the small-molecule AXL inhibitors to reproduce this phenotype makes it more likely that this modulation stems from off-target shRNA effects. Altogether, our results suggest that AXL expression may be sufficient to confer acquired resistance to MAPK pathway inhibitors, but may not be necessary for maintenance of resistance. Although AXL expression may nonetheless contribute to the intrinsic resistant phenotype in these melanoma cells, AXL does not seem to be the sole or limiting resistance effector in this setting. We therefore returned to the broader differences in transcriptional state that exist among lines with differential sensitivity to MAPK pathway inhibitors.

The foregoing experiments raised the possibility that distinct melanoma cell states characterized by specific transcriptional profiles might underpin intrinsic resistance to MAPK pathway inhibition in BRAF^{V600}-mutant melanoma. One possible explanation for the existence of these transcriptional states is that they might arise from distinct precursor cells. To test this possibility, we analyzed whether the transcriptional states could both be established from immortalized primary human melanocytes. At baseline, immortalized melanocytes expressed high levels of both MITF and its target genes, reminiscent of MITF-high/NF-κB–low melanoma cell lines. In addition, expression of NF-κB–associated signatures and marker genes was low in these melanocytes (Fig. 4A and B). As expected, introduction of BRAF^{V600E} into immortalized melanocytes augmented ERK phosphorylation (Fig. 4B and Supplementary Fig. S14). Consistent with prior observations (20), ectopic BRAF^{V600E} also abrogated MITF expression [at both the transcriptional (Fig. 4A) and protein levels (Fig. 4B and Supplementary Fig. S14)] and MITF transcriptional activity (as measured by an expression signature of MITF activity as well as levels of individual MITF target genes; Fig. 4A and B and Supplementary Fig. S14). Surprisingly, expression of BRAF^{V600E} also induced NF-κB pathway activation, as measured by expression of NF-κB–driven transcriptional signatures (Fig. 4A), RELA phosphorylation (Fig. 4B and Supplementary Fig. S14), and expression of markers such as AXL and NRP1 (Fig. 4A and B and Supplementary

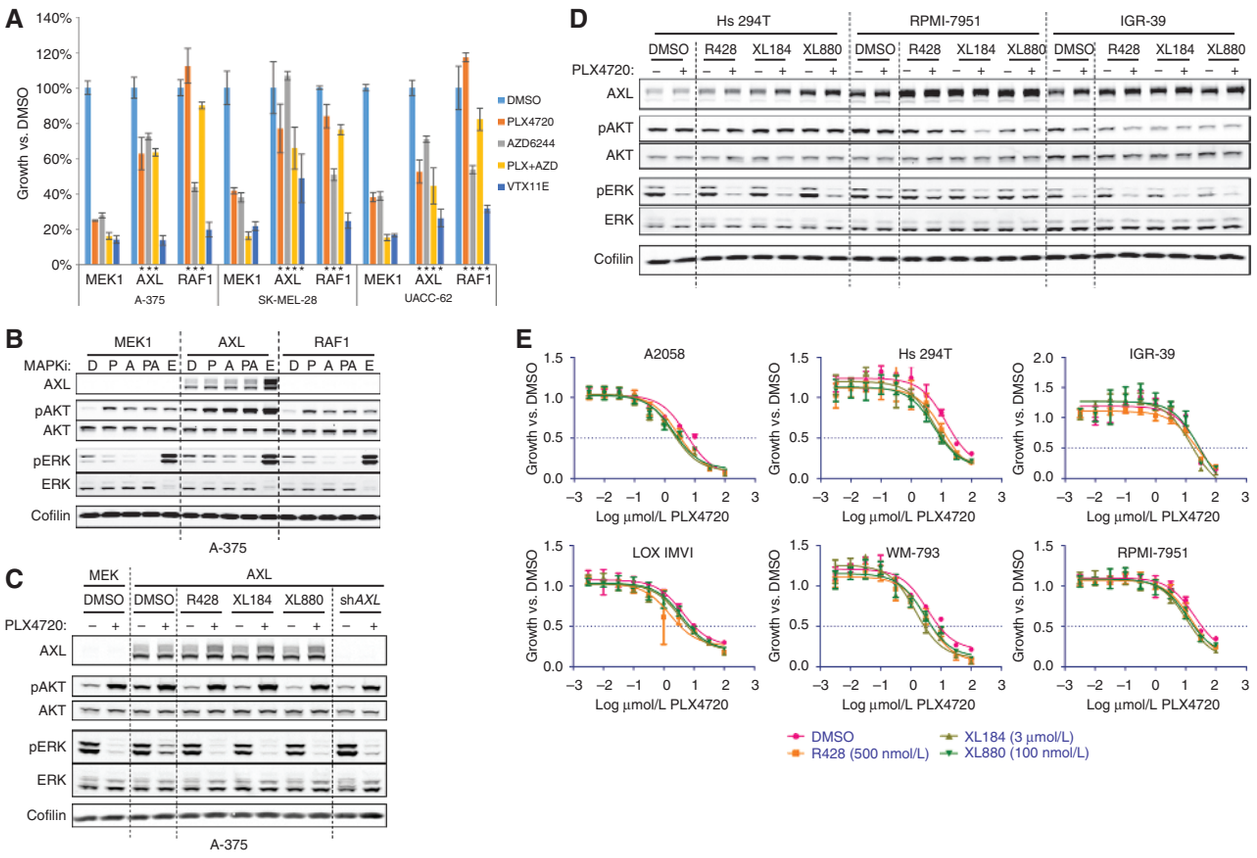

Figure 3. AXL is not necessary for maintenance of intrinsic resistance. **A,** effects of AXL overexpression on survival of drug-sensitive BRAF^{V600}-mutant melanoma cell lines following 4-day treatment with PLX4720 (RAFi, 2 μmol/L), AZD6244 (MEKi, 200 nmol/L), PLX4720 + AZD6244, or VTX11E (ERKi, 2 μmol/L). MEK1 is a negative control; RAF1 is a positive control for RAFi resistance. Data are mean ± standard deviation. Asterisks beneath graph indicate $P < 0.01$ (two-tailed *t* test) relative to the same cell line, expressing MEK1, and treated with the same drug. **B,** effects of AXL overexpression on phosphorylation of AKT and maintenance of ERK phosphorylation following overnight treatment with MAPK pathway inhibitors. D, DMSO; P, 2 μmol/L PLX4720; A, 200 nmol/L AZD6244; PA, PLX4720 + AZD6244; and E, VTX11E, 2 μmol/L. MEK1 is a negative control; RAF1 is a positive control for pERK reactivation following RAFi treatment. **C,** effects of AXL inhibitors on induction of pAKT and rescue of pERK following AXL overexpression. R428, 500 nmol/L; XL184, 3 μmol/L; XL880, 100 nmol/L; in the presence or absence of 2 μmol/L PLX4720. sh*AXL* is a positive control. **D,** effects of AXL inhibitors on pAKT and pERK levels in intrinsically resistant cell lines in the presence or absence of PLX4720. **E,** effects of AXL inhibitors on intrinsic resistance to PLX4720.

Fig. S14). Thus, short-term overexpression of BRAF^{V600E} in melanocytes suppressed MITF activity, induced NF-κB activity, and produced an MITF-low/NF-κB–high expression pattern reminiscent of intrinsically resistant melanomas.

We also examined melanocytes that ectopically expressed BRAF^{V600E} over a prolonged time period (8–12 weeks) and at near-endogenous levels. Comparable results were obtained in this context (Fig. 4C), suggesting that these phenotypic patterns are durable and not simply an artifact of acute, supra-physiologic oncogene expression. A constitutively active variant of MEK1 (MEK1^{DD}) similarly suppressed MITF and upregulated AXL, whereas MAPK pathway inhibitors largely reversed these effects (Fig. 4A and B and Supplementary Fig. S14). These results suggest that aberrant MAPK pathway signaling is both necessary and sufficient for induction of these transcriptional changes following gain of BRAF^{V600E}. In addition, BRAF^{V600E}-mediated induction of AXL, but not MITF loss, was partially antagonized by an IκBα super-repressor (Supplementary Fig. S15), suggesting that the NF-κB activation induced by BRAF^{V600E} may partially contribute to expression of marker genes associated with the NF-κB–high transcriptional state in this context. Altogether, these results suggest that the MITF-low/NF-κB–high phenotype can, in some circumstances, be at least partially induced by oncogenic MAPK signaling, including gain of BRAF^{V600E}.

Although BRAF^{V600E} induced a transcriptional phenotype suggestive of an MITF-low/NF-κB–high cell state in melanocytes *in vitro* (Fig. 4A–C and Supplementary Fig. S14; ref. 20), the majority of BRAF^{V600}-mutant melanoma cells exhibit the opposite (i.e., MITF-high/NF-κB–low) cell state both *in vitro* and *in vivo*. Because MITF expression is a prominent feature of the "typical" BRAF^{V600}-mutant melanoma cell state, we hypothesized that concomitant MITF dysregulation might antagonize BRAF^{V600E}-mediated induction of an alternative, NF-κB–high cell state. To test this possibility, we ectopically expressed MITF in melanocytes simultaneously with either BRAF^{V600E} or MEK1^{DD}. In melanocytes endogenously expressing high levels of MITF, ectopic MITF expression only minimally altered MITF levels. However, in the setting of ectopic BRAF^{V600E} or MEK1^{DD} expression, where MITF levels are reduced, even a partial restoration of MITF levels by ectopic MITF expression blocked

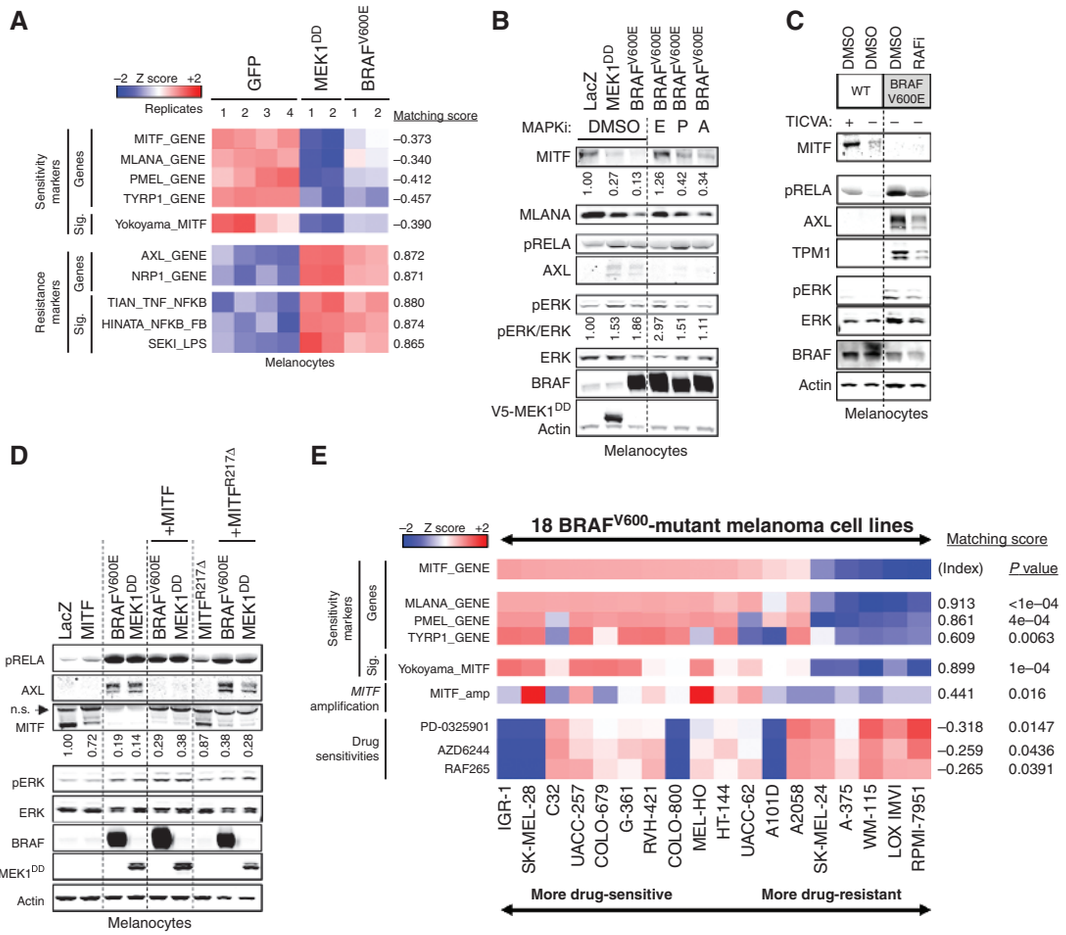

Figure 4. Establishment of transcriptional class distinction in melanocytes. **A,** effects of aberrant MAPK pathway activation on melanocyte whole-genome expression profiles. **B,** effects of aberrant MAPK pathway activation on markers of the MITF-high and NF-κB–high classes; E, VTX11E (ERKi); P, PLX4720 (RAFi); A, AZD6244 (MEKi), all overnight at 2 μmol/L. **C,** effects of chronic BRAF^{V600E} expression on markers of the MITF-high and NF-κB–high classes. Experiments were performed in TICVA medium (+) or Ham's F10 (–) as indicated. **D,** effect of MITF overexpression on MAPK pathway–induced expression changes. n.s., nonspecific band. **E,** relationship between MITF expression levels and *MITF* amplification in melanoma cell lines.

the ability of BRAF^{V600E} or MEK1^{DD} to induce AXL expression, one of the defining features of the NF-κB–high state (Fig. 4D and Supplementary Fig. S16). Thus, following gain of aberrant MAPK pathway activation, the continued presence of MITF may blunt the transition into the NF-κB–high transcriptional state. This effect was dependent on the ability of MITF to bind DNA, as a DNA binding–deficient mutant [MITF(R217Δ)] was unable to suppress AXL expression (Fig. 4D and Supplementary Fig. S16). Consistent with these data, we found an enrichment of *MITF* amplification in those BRAF^{V600}-mutant melanoma cell lines retaining an MITF-high/NF-κB–low transcriptional state (Fig. 4E). These observations raise the possibility that, in the context of BRAF^{V600E}, concomitant MITF dysregulation contributes to maintenance of an MITF-high/NF-κB–low state.

Collectively, these data imply that, in at least some settings, it is possible to establish both MITF-low/NF-κB–high and MITF-high/NF-κB–low cellular states from the same precursor melanocyte. They also raise the possibility that a key determinant of transcriptional states associated with resistance versus sensitivity is the balance between, on the one hand, BRAF^{V600E}-mediated MAPK pathway activation and subsequent NF-κB induction, and, on the other, sustained MITF expression.

Because both MITF and NF-κB can influence the establishment of distinct cell states in melanocytes, we next investigated whether these factors could also affect maintenance of these states in established melanoma cell lines. Specifically, we hypothesized that induction of NF-κB could modulate a cell line away from an MITF-high state toward an MITF-low state. Because our aforementioned experiments suggested that intrinsic resistance might result from a global transcriptional state as opposed to expression of individual resistance effector(s), we further predicted that this perturbation of transcriptional state should alter drug sensitivity. Whereas previous analyses demonstrated an association between NF-κB transcriptional state and resistance, here we sought to query whether manipulation of transcriptional state could causally affect drug resistance. We induced NF-κB activity in sensitive cell lines by treating them with the NF-κB agonist TNFα, which led to increased phosphoactivation of the NF-κB transcription factor RELA (Fig. 5A). Following this induction of NF-κB activity, we observed a decrease in both

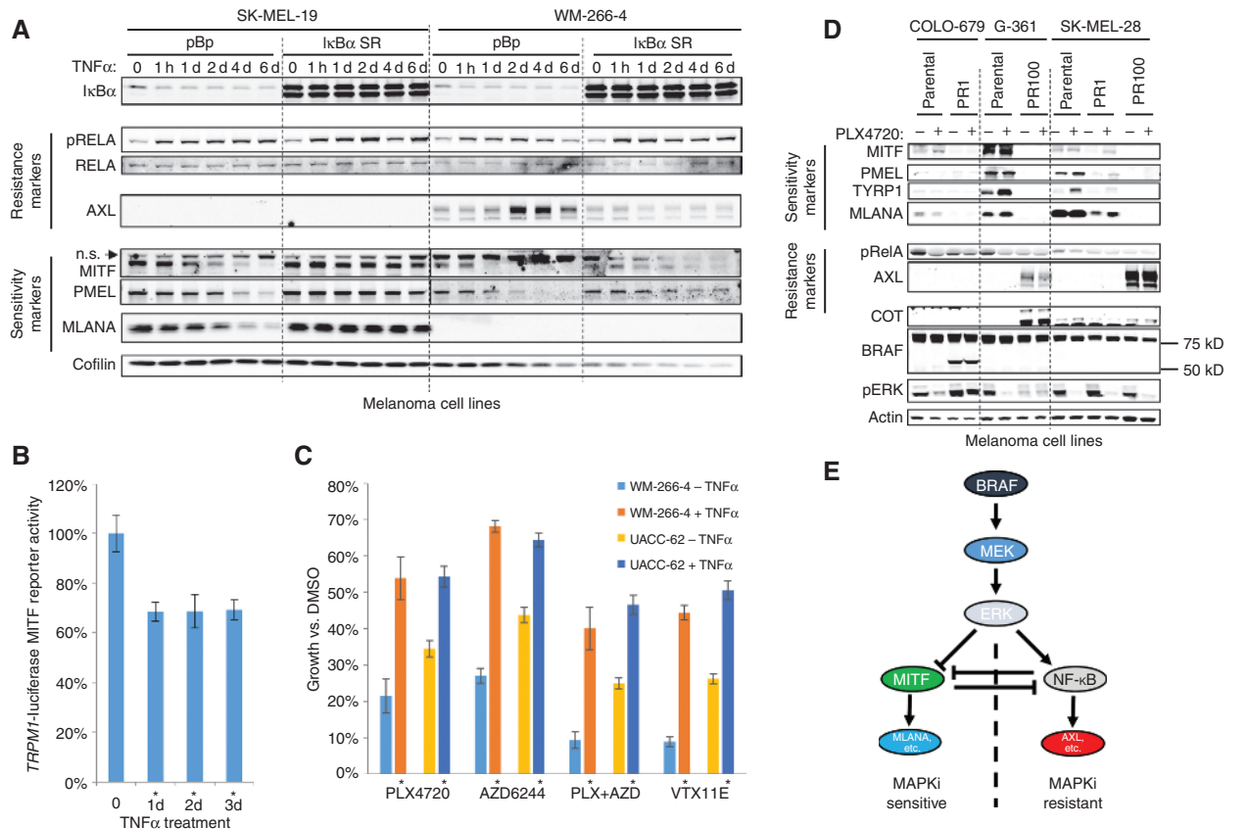

Figure 5. Plasticity of transcriptional class distinction in melanoma cell lines. **A,** effect of TNFα (25 ng/mL), with or without concomitant IκBα super-repressor expression, on RELA phosphorylation and expression of resistance markers, MITF, and MITF target genes. n.s., nonspecific band. **B,** effect of TNFα (25 ng/mL) on MITF transcriptional activity, as measured in an SK-MEL-5 melanoma cell line stably expressing a *TRPM1*-luciferase MITF reporter construct. *, $P < 0.001$ (two-tailed *t* test) relative to no TNFα treatment. **C,** effect of TNFα (30 ng/mL) on sensitivity to the indicated MAPK pathway inhibitors. PLX4720, 2 μmol/L; AZD6244, 200 nmol/L; VTX11E, 2 μmol/L. *, $P < 0.001$ (two-tailed *t* test) relative to the same cell line and same MAPKi without TNFα. **D,** comparison of expression of MITF, AXL, and associated marker genes in parental (sensitive) and cultured-to-resistant melanoma cell lines, with or without 24-hour treatment with PLX4720 (2 μmol/L). PR1 and PR100 denote independent derivations of a resistant subclone. **E,** model of transcriptional state distinction in melanoma.

MITF expression and MITF activity (as measured by levels of the MITF target gene *PMEL*; Fig. 5A). To further verify the effects of NF-κB on MITF transcriptional activity, we used SK-MEL-5 cells stably expressing a luciferase reporter under the control of the promoter of *TRPM1*, a known MITF target gene. This system has previously been used as a readout of MITF transcriptional activity (32). Using this approach, we observed a reduction in MITF transcriptional reporter activity following TNFα treatment (Fig. 5B), the magnitude of which was comparable with the reduction in protein expression of MITF target genes (Supplementary Fig. S17A). In some cell lines, TNFα not only suppressed MITF but also induced expression of resistance markers including AXL (Fig. 5A and Supplementary Fig. S17B). In addition, blockade of NF-κB activity with the IκBα super-repressor abrogated these TNFα-mediated expression changes (Fig. 5A), confirming that NF-κB signaling was necessary for these transcriptional changes. Thus, NF-κB activation seemed to promote a transition from an MITF-high/NF-κB–low to an MITF-low/NF-κB–high transcriptional phenotype.

If activation of NF-κB by TNFα perturbs cells away from an MITF-high/NF-κB–low state toward an MITF-low/NF-κB–high state, and if cell state controls drug sensitivity, we reasoned that the same stimulus should also confer phenotypic drug resistance. Indeed, we observed that TNFα led to resistance to inhibition of RAF and MEK, singly or in combination, as well as ERK (Fig. 5C and Supplementary Fig. S18; refs. 33, 34). Thus, NF-κB activation can perturb a sensitive, MITF-high/NF-κB–low state toward a state that is not only MITF-low/NF-κB–high but also functionally resistant to MAPK pathway inhibition. Crucially, therefore, perturbing the cellular transcriptional state can result in a phenotypic alteration in drug sensitivity. On this basis, it seems that NF-κB activity is not simply a marker of the MITF-low resistant state, but rather is functionally sufficient to induce it.

Finally, because MAPK pathway hyperactivation could promote establishment of the MITF-low/NF-κB–high state in melanocytes, we wondered whether therapeutic MAPK pathway inhibition in $BRAF^{V600}$-mutant melanomas would affect maintenance of this state. To test this hypothesis, we cultured four MITF-high, MAPK pathway inhibitor–sensitive melanoma cell lines continuously in PLX4720 until a resistant population emerged (Supplementary Fig. S19). Interestingly, resistant cells showed diminished MITF expression and MITF

transcriptional activity (as measured by levels of MITF target genes *TYRP1*, *MLANA*, and *PMEL*; 4/4 lines) and gain of AXL expression (2/4 lines; Fig. 5D). These results suggest that in some contexts, MITF-high/NF-κB–low melanomas can transition toward an MITF-low/NF-κB–high state during acquisition of resistance. These changes were observed even in clones that had also gained other known mechanisms of resistance [Fig. 5D; e.g., COT expression and p61 BRAF splice variant (10, 12)]. This finding implies that transition toward an MITF-low/NF-κB–high state is not mutually exclusive with acquisition of other known resistance effectors—an emerging theme in resistance to targeted therapeutics (35). Moreover, this finding suggests that the MITF-low/NF-κB–high state, although certainly associated with intrinsic resistance, can be also observed in the context of acquired resistance. Thus, the MITF-low/NF-κB–high transcriptional phenotype may generally signify diminished dependence on the MAPK pathway. Melanomas that begin in this MITF-low/NF-κB–high state before treatment are likely to be intrinsically resistant to MAPK pathway inhibition, whereas melanomas that transition into this state during treatment can exhibit acquired resistance. Cumulatively, these findings demonstrate that, even in melanoma cell lines, the transcriptional states associated with sensitivity and resistance remain plastic; moreover, maintenance of these states in cell lines can be perturbed by the same mediators that govern establishment of these states in melanocytes (Fig. 5E).

DISCUSSION

The majority of $BRAF^{V600}$-mutant melanomas are profoundly dependent on the RAF–MEK–ERK signaling cascade. This vulnerability has been exploited clinically with the development of pharmacologic RAFi and MEKi. However, the efficacy of these drugs is limited both by relapse following an initial response (acquired resistance) and by the initial indifference of some $BRAF^{V600}$-mutant melanomas to these inhibitors (intrinsic resistance). Multiple studies have elucidated mechanisms of acquired resistance to MAPK pathway inhibitor therapy, largely converging on reactivation of the MAPK pathway (7, 10–16). Although recent work has identified stromal HGF secretion as one mechanism of intrinsic resistance (17, 18), less has been known about whether there also exist cell-autonomous determinants of this phenotype.

In this study, we used a collection of $BRAF^{V600}$-mutant melanoma cell lines displaying a spectrum of sensitivity to MAPK pathway inhibitors to identify two transcriptional states in $BRAF^{V600}$-mutant melanoma: one characterized by high MITF expression and transcriptional activity that is sensitive to MAPK pathway inhibition, and another that exhibits low MITF expression and activity, high NF-κB activity, and resistance to MAPK pathway inhibition. The MITF-low/NF-κB–high state seems specifically resistant to MAPK pathway inhibition, rather than globally drug-tolerant, as cross-resistance to other classes of therapeutics was not observed. Moreover, such a transcriptional class distinction is reminiscent of prior work identifying two differential gene expression classes in melanoma (26, 27). However, both the mechanistic basis and the therapeutic implications of this two-class distinction have been largely uncharacterized; in particular, it has not previously been associated with differential response to vemurafenib or dabrafenib/trametinib in the setting of $BRAF^{V600}$ mutation. Conversely, although the phenomenon of intrinsic sensitivity/resistance to MAPK pathway inhibitors has more recently become evident, a cell-intrinsic mechanistic basis for this phenomenon has remained largely unknown. Thus, our current work may unify and extend two previously described phenomena in melanoma by proposing gene expression reciprocity between MITF and NF-κB as a mechanistic determinant of intrinsic resistance.

Our data suggest that the origin of these two distinct states in melanocytes can be controlled by the relative balance of aberrant MAPK activation (leading to NF-κB activation and the MITF-low/NF-κB–high state) and sustained MITF expression and activity (leading to the MITF-high/NF-κB–low state). Because we and others have shown that introduction of $BRAF^{V600E}$ into melanocytes can lead to loss of MITF expression and activity, it may seem surprising that the majority of $BRAF^{V600}$-mutant melanomas retain MITF expression and activity and low levels of NF-κB activity. Of note, we also show that chronic MAPK pathway inhibition led some melanoma lines to transition to an MITF-low/NF-κB–high state. Although one possible explanation for this finding is simply outgrowth of a preexisting resistant subpopulation, it may also suggest that not all melanomas preserve the same relationship between MAPK signaling and MITF levels as observed in melanocytes.

An additional possible explanation for the maintenance of MITF expression in $BRAF^{V600}$-mutant melanomas is our finding that dysregulation of MITF—for example, by ectopic expression—can impair induction of the NF-κB–high state. Indeed, we observed that *MITF* amplification was enriched in the MITF-high cell lines relative to the NF-κB–high cell lines, suggesting that this genomic alteration may contribute to the ability of some melanomas to maintain MITF following acquisition of $BRAF^{V600E}$. In addition, recent work has shown that, in $BRAF^{V600}$-mutant melanoma cell lines, enforced (rather than endogenous) MITF activity is permissive for cellular proliferation following MAPK pathway inhibition (36). This result is consistent with our finding that endogenous levels of MITF predict sensitivity to MAPK pathway inhibition. Because endogenous MITF is regulated by the MAPK pathway, endogenous MITF levels function as a proxy for MAPK pathway dependency, whereas in MITF-low melanomas, additional transcription factors may permit MAPK-independent cell-cycle progression. In contrast to endogenous MITF, however, exogenous MITF is not regulated by the MAPK pathway and therefore allows MAPK-independent cellular proliferation.

In our initial analysis, the MITF-low/NF-κB–high subgroup of melanomas was identified as exhibiting resistance to single-agent RAF or MEK inhibition. One recent strategy for enhancing the response to MAPK pathway inhibition has been to combine RAF and MEK inhibition (6). However, the MITF-low/NF-κB–high melanomas were also resistant to combined RAF and MEK inhibition as well as to ERK inhibition. This resistance was apparent despite robust biochemical evidence for MAPK pathway inhibition, arguing that these melanomas may be largely indifferent to MAPK pathway blockade. Our findings therefore raise the possibility that combination (e.g., RAF–MEK) or additional downstream (e.g., ERK) inhibition of the MAPK pathway may not achieve durable therapeutic control of at least some $BRAF^{V600}$-mutant melanomas.

These analyses suggested that the MITF-low/NF-κB–high state is associated with a diminished sensitivity to MAPK pathway inhibition. For this reason, melanoma cells that begin in this state before MAPK pathway inhibitor therapy show intrinsic resistance to such treatment. We also found, however, that these transcriptional states may not be permanently fixed, but rather can exhibit a degree of plasticity during therapy. When MITF-high cell lines were cultured in PLX4720 to resistance, a transition to an MITF-low/NF-κB–high state was observed. Direct stimulation of the NF-κB pathway by TNFα recapitulated these expression changes in an NF-κB–dependent fashion. Moreover, this change of transcriptional state by NF-κB activation also induced phenotypic resistance to MAPK pathway inhibitors, thus providing direct evidence for the key role of the NF-κB pathway in establishing the resistant cellular state. Intriguingly, when cultured to resistance to single-agent RAF inhibition, melanoma cells also acquired cross-resistance to inhibition of MEK, RAF and MEK in combination, and ERK. This state transition occurred together with the acquisition of other known effectors of acquired resistance, including COT and the p61 BRAF splice variant. This apparent plasticity between the MITF-high/NF-κB–low and MITF-low/NF-κB–high states may therefore accompany other acquired resistance effectors that converge on the MAPK pathway. Moreover, this finding may implicate a transition between these cellular states in the acquisition of resistance to RAFi/MEKi. An important feature of this model is that the MITF-low/NF-κB–high transcriptional state is not restricted to either an intrinsic or acquired resistance context, but rather is fundamentally a state of diminished dependency on the MAPK pathway. Thus, whereas transcriptional state before therapy may influence intrinsic resistance, the ability to modulate transcriptional state during therapy may contribute to acquired resistance.

Because MITF-low/NF-κB–high melanomas can exhibit resistance to MAPK pathway inhibition, the identification of alternative therapeutic avenues for these tumors is of great interest. *AXL*, one gene associated with the NF-κB–high resistant state, has previously been shown to be sufficient to cause acquired MAPKi resistance. However, efforts to render intrinsically resistant melanomas sensitive to MAPK pathway inhibition through inhibition of AXL *in vitro* suggested that AXL was not necessary for the maintenance of intrinsic resistance—a finding consistent with the observation that these cell lines were resistant to ERK inhibition, a phenotype that AXL alone did not robustly affect. Thus, intrinsic resistance seems to be not simply a consequence of AXL expression, but rather due to a more fundamental cell state distinction that happens to involve AXL expression. For this reason, the identification of new pharmacologic vulnerabilities in this resistant state—whether singly or in combination with MAPK pathway inhibition—will be a high priority for future investigation.

In summary, our findings reveal that resistance to MAPK pathway inhibition in $BRAF^{V600}$-mutant melanoma can be associated with a distinct transcriptional state, both *in vitro* and in human tumors. The establishment and maintenance of these states seems linked to aberrant MAPK pathway activation, NF-κB induction, and MITF dysregulation. This class distinction may aid future efforts in $BRAF^{V600}$-mutant melanoma to predict treatment response and identify new therapeutic strategies for patients who fail to benefit from RAF/MEK inhibition.

METHODS

Cell Culture

Cell lines obtained from the American Type Culture Collection, the National Cancer Institute (Bethesda, MD), and Deutsche Sammlung von Mikroorganismen und Zellkulturen, which verify identity by short tandem repeat profiling, were passaged <6 months following receipt. SK-MEL-5-*TRPM1*-luciferase cells were a gift of David E. Fisher (Massachusetts General Hospital, Boston, MA). Cells were maintained (unless otherwise indicated) in medium supplemented with 10% FBS (Gemini Bio-Products) and 1% penicillin/streptomycin. The following cell lines were maintained in RPMI-1640: A-375, COLO-679, RVH-421, SK-MEL-5, SK-MEL-19, SK-MEL-28, UACC-62, WM-983B, WM-793, LOX IMVI, and all short-term cultures; DMEM: WM-88, WM-266-4, G-361, A2058, and Hs 294T; MEM: RPMI-7951; and DMEM with 15% FBS: IGR-39.

MITF Reporter Cell Line

SK-MEL-5-*TRPM1*-luciferase cells were a kind gift of David E. Fisher, and the stable derivation of this line will be described in a forthcoming article. Cells were seeded at 5,000 cells per well in duplicate in 96-well clear- and white-bottomed plates. Beginning the day after seeding, cells were treated with 25 ng/mL final TNFα for the indicated time points. Four days after seeding, viability was read out from clear-bottomed plates using CellTiter-Glo (1:5 final dilution) and luciferase activity from white-bottomed plates using ONE-Glo (Promega; 1:2 final dilution). Luciferase activity was then normalized to viability and expressed as a percentage of activity in untreated cells.

Inhibitors

PLX4720, AZD6244, XL184, and XL880 were purchased from Selleck Chemicals. R428 was purchased from Symansis. VTX11E was synthesized as previously reported (24). All small molecules were dissolved in DMSO. For Western blot analysis following MAPK pathway inhibitor treatment, all cells were seeded in parallel and allowed to proliferate for 5 days, with indicated drugs added for the indicated lengths of time before simultaneous final harvest.

GI_{50} Determination

For determining the half-maximal growth inhibitory concentration (GI_{50}), lines were seeded in 96-well format. The day after plating, if applicable, recombinant human TNFα [Cell Signaling Technology (CST) 8902SC, 25 ng/mL final] or AXL inhibitors (at indicated dilutions) were added. Cells were then drugged with serial dilutions of indicated inhibitors to give final concentrations ranging from 100 μmol/L to 31.62 nmol/L (PLX4720 and VTX11E) or 31.62 μmol/L to 10 nmol/L (AZD6244), in half-log increments. For combined PLX4720 and AZD6244 treatment, an equitoxic combination of doses was used, starting at 100 μmol/L PLX4720 + 31.62 μmol/L AZD6244. Four days later, cellular viability was assessed using CellTiter-Glo (Promega). GI_{50} calculations were performed in GraphPad Prism; for AZD6244, floor value was set to 0. In Fig. 1C and Supplementary Fig. S4A, "relative sensitivity" was calculated by dividing the GI_{50} of a given drug in a given cell line by the median GI_{50} of the same drug in the sensitive group of cell lines.

Constructs

MEK1, RAF1, AXL (clone 7F12), MITF-M, LacZ, $BRAF^{V600E}$, and $MEK1^{DD}$ in lentiviral vectors pLX304-Blast-V5 or pLX980-Blast-V5 were from The RNAi Consortium (Broad Institute, Cambridge, MA). The retroviral IκBα super-repressor construct has been previously published (37).

Viral Infections

Unless otherwise indicated, all viral infections were carried out the day after seeding in 4 μg/mL final polybrene with centrifugation for 60 minutes at 2,250 rpm (1,178 × *g*) at 30°C, with an immediate medium change following infection. Viral dilutions were 1:50 for

shRNA lentiviruses, 1:10 for ORF lentiviruses, and 1:3 for retroviruses.

Inhibitor Treatment Following ORF Infection

For Western blot analysis, 4 days after infection with the indicated ORF lentivirus, medium was changed to fresh medium plus DMSO or small molecules as indicated, with harvest the next day. For viability assays following ORF infections, cells were seeded in 96-well format at the following densities: A-375, 900; SK-MEL-28, 1,100; and UACC-62, 2,750. The next day, cells were infected as described above; 3 days later, inhibitors were added at the indicated concentrations. Four days after inhibitor treatment, viability was read out using CellTiter-Glo.

TNFα Time Course with IκBα Super-Repressor

Each of the 2 days following seeding, cells were infected overnight with indicated retrovirus, with an 8-hour recovery between infections. The day after the second infection, medium was changed to fresh medium plus 1 μg/mL final puromycin, and cells were stimulated for the 6-day TNFα time point (25 ng/mL final). Subsequent time points were stimulated as indicated, and all time points were harvested in parallel.

Primary Melanocytes

Primary melanocytes were grown in TICVA medium [Ham's F-10 (CellGro), 7% FBS, 1% penicillin/streptomycin, 2 mmol/L glutamine (CellGro), 100 μmol/L IBMX, 50 ng/mL TPA (12-O-tetradecanoylphorbol-13-acetate), 1 mmol/L 3′,5′-cyclic AMP dibutyrate (dbcAMP; Sigma), and 1 μmol/L sodium vanadate]. Lentiviral infections were performed as described above for 1 hour (for Western blot analysis) or overnight (for expression profiling). For Western blot analysis, cells were switched to Ham's F10 plus 10% FBS following introduction of $BRAF^{V600E}$ or $MEK1^{DD}$, and lysates were harvested as described in Supplementary Methods. For expression profiling, cells were selected following infection in 10 μg/mL puromycin for 4 days and propagated stably before RNA harvesting using the RNeasy MiniPrep Kit according to the manufacturer's protocols (Qiagen). RNA quality was assessed using a 2100 Bioanalyzer (Agilent) before expression profiling on an Affymetrix U133+ PM array according to the manufacturer's protocols.

Gene Expression and Pharmacologic Analyses

Gene expression (robust multi-array average normalized using ENTREZG v15 CDF), drug sensitivity (GI_{50} values for Fig. 1A and Supplementary Fig. S1, activity area for Figs. 1B and 4E), and genotyping data for $BRAF^{V600}$-mutant melanoma cell lines were from the CCLE (19). Pearson correlation coefficients (r) were computed between gene expression values and PLX4720 GI_{50} values as well as between GI_{50} values for various small molecules and MITF expression values. For Fig. 4E, gene expression, genotyping, and copy-number data were from the Wellcome Trust/Sanger COSMIC Cell Lines Project (38); drug sensitivity was from the CCLE. Gene expression and genotyping data for melanoma short-term cultures (Fig. 1C) were from Lin and colleagues (39); expression data were collapsed to maximum probe value per gene using GSEA Desktop. Genotyping and gene expression data for melanoma tumors in Fig. 2A were from The Cancer Genome Atlas (https://tcga-data.nci.nih.gov/tcga/).

MITF and AXL Staining

For immunocytochemistry, 5 days after seeding, cells were scraped in cold PBS, formalin-fixed, paraffin-embedded, and processed as below. For immunohistochemistry, 4-μm sections of formalin-fixed, paraffin-embedded specimens were heated at 60°C, deparaffinized in xylene, and hydrated in a series of ethanol dilutions. Epitope retrieval was done by microwaving (5 minutes at 850 W, 15 minutes at 150 W) in 10 mmol/L Tris–EDTA buffer pH 9.0. Slides were blocked 10 minutes in 3% BSA in TBST (Tris pH 7.6, 0.05% Tween-20). Primary antibodies were as follows: MITF, 1:100 in 3% BSA in TBST, clone D5 (Dako M3621); AXL, 1:100 in 3% BSA in TBST, clone C89E7 (CST 8661). Slides underwent 10-minute peroxidase block in 3% H_2O_2. Secondary antibodies were: goat anti-mouse IgG-HRP (Bio-Rad 170-6516), 1:200 in 3% BSA in TBST; Dako EnVision anti-rabbit (K4003, ready-to-use). Slides were developed with DAB+ (Dako K3468) for 10 minutes and counterstained for 1 minute with hematoxylin (Vector H-3401) before dehydration and mounting. Slides were imaged on an Olympus BX51 microscope with Olympus DP25 camera using Olympus WHN10X-H/22 oculars, Olympus UPlan FL N −20x/0.50 and −40x/0.50 objectives, an Olympus DP25 camera, and images acquired using Olympus DP2-TWAIN software and Adobe Photoshop 7.0. Slides were scored for intensity and distribution of AXL and MITF by a dermatopathologist blinded to clinical outcome.

Disclosure of Potential Conflicts of Interest

W.C. Hahn has received a commercial research grant from Novartis and is a consultant/advisory board member of the same. J.A. Wargo has received honoraria from the Speakers Bureau of Dava Oncology. L.A. Garraway has received a commercial research grant from Novartis, has ownership interest (including patents) in Foundation Medicine, and is a consultant/advisory board member of Millennium, Novartis, and Boehringer Ingelheim. No potential conflicts of interest were disclosed by the other authors.

Authors' Contributions

Conception and design: D.J. Konieczkowski, C.M. Johannessen, R. Haq, L.A. Garraway

Development of methodology: D.J. Konieczkowski, O. Abudayyeh, M. Barzily-Rokni, J.P. Mesirov, W.C. Hahn, L.A. Garraway

Acquisition of data (provided animals, acquired and managed patients, provided facilities, etc.): D.J. Konieczkowski, C.M. Johannessen, J.W. Kim, Z.A. Cooper, A. Piris, D.T. Frederick, R. Straussman, J.A. Wargo

Analysis and interpretation of data (e.g., statistical analysis, biostatistics, computational analysis): D.J. Konieczkowski, C.M. Johannessen, O. Abudayyeh, Z.A. Cooper, A. Piris, J.P. Mesirov, K.T. Flaherty, J.A. Wargo, P. Tamayo, L.A. Garraway

Writing, review, and/or revision of the manuscript: D.J. Konieczkowski, C.M. Johannessen, O. Abudayyeh, J.W. Kim, A. Piris, D.T. Frederick, W.C. Hahn, K.T. Flaherty, J.A. Wargo, L.A. Garraway

Administrative, technical, or material support (i.e., reporting or organizing data, constructing databases): C.M. Johannessen, D.T. Frederick

Study supervision: C.M. Johannessen, L.A. Garraway

Creation of BRAF inhibitor cultured-to-resistant melanoma cell lines: R. Straussman

Contribution of key materials: D.E. Fisher

Grant Support

D.J. Konieczkowski was supported by training grant T32GM007753 from the National Institute of General Medical Sciences. L.A. Garraway was supported by grants from the NIH, NCI, Melanoma Research Alliance, Starr Cancer Consortium, and the Dr. Miriam and Sheldon G. Adelson Medical Research Foundation.

Received July 24, 2013; revised April 11, 2014; accepted April 18, 2014; published OnlineFirst April 25, 2014.

REFERENCES

1. Davies H, Bignell GR, Cox C, Stephens P, Edkins S, Clegg S, et al. Mutations of the BRAF gene in human cancer. Nature 2002;417:949–54.
2. Hodis E, Watson IR, Kryukov GV, Arold ST, Imielinski M, Theurillat JP, et al. A landscape of driver mutations in melanoma. Cell 2012;150:251–63.

3. Solit DB, Garraway LA, Pratilas CA, Sawai A, Getz G, Basso A, et al. BRAF mutation predicts sensitivity to MEK inhibition. Nature 2006;439:358–62.
4. Flaherty KT, Puzanov I, Kim KB, Ribas A, McArthur GA, Sosman JA, et al. Inhibition of mutated, activated BRAF in metastatic melanoma. N Engl J Med 2010;363:809–19.
5. Chapman PB, Hauschild A, Robert C, Haanen JB, Ascierto P, Larkin J, et al. Improved survival with vemurafenib in melanoma with BRAF V600E mutation. N Engl J Med 2011;364:2507–16.
6. Flaherty KT, Infante JR, Daud A, Gonzalez R, Kefford RF, Sosman J, et al. Combined BRAF and MEK inhibition in melanoma with BRAF V600 mutations. N Engl J Med 2012;367:1694–703.
7. Emery CM, Vijayendran KG, Zipser MC, Sawyer AM, Niu L, Kim JJ, et al. MEK1 mutations confer resistance to MEK and B-RAF inhibition. Proc Natl Acad Sci U S A 2009;106:20411–6.
8. Wagle N, Van Allen EM, Treacy DJ, Frederick DT, Cooper ZA, Taylor-Weiner A, et al. MAP kinase pathway alterations in BRAF-mutant melanoma patients with acquired resistance to combined RAF/MEK inhibition. Cancer Discov 2014;4:61–8.
9. Van Allen EM, Wagle N, Sucker A, Treacy DJ, Johannessen CM, Goetz EM, et al. The genetic landscape of clinical resistance to RAF inhibition in metastatic melanoma. Cancer Discov 2014;4:94–109.
10. Poulikakos PI, Persaud Y, Janakiraman M, Kong X, Ng C, Moriceau G, et al. RAF inhibitor resistance is mediated by dimerization of aberrantly spliced BRAF(V600E). Nature 2011;480:387–90.
11. Montagut C, Sharma SV, Shioda T, McDermott U, Ulman M, Ulkus LE, et al. Elevated CRAF as a potential mechanism of acquired resistance to BRAF inhibition in melanoma. Cancer Res 2008;68:4853–61.
12. Johannessen CM, Boehm JS, Kim SY, Thomas SR, Wardwell L, Johnson LA, et al. COT drives resistance to RAF inhibition through MAP kinase pathway reactivation. Nature 2010;468:968–72.
13. Nazarian R, Shi H, Wang Q, Kong X, Koya RC, Lee H, et al. Melanomas acquire resistance to B-RAF(V600E) inhibition by RTK or N-RAS upregulation. Nature 2010;468:973–7.
14. Maertens O, Johnson B, Hollstein P, Frederick DT, Cooper ZA, Messiaen L, et al. Elucidating distinct roles for NF1 in melanomagenesis. Cancer Discov 2013;3:338–49.
15. Whittaker SR, Theurillat JP, Van Allen E, Wagle N, Hsiao J, Cowley GS, et al. A genome-scale RNA interference screen implicates NF1 loss in resistance to RAF inhibition. Cancer Discov 2013;3:350–62.
16. Lito P, Pratilas CA, Joseph EW, Tadi M, Halilovic E, Zubrowski M, et al. Relief of profound feedback inhibition of mitogenic signaling by RAF inhibitors attenuates their activity in BRAFV600E melanomas. Cancer Cell 2012;22:668–82.
17. Straussman R, Morikawa T, Shee K, Barzily-Rokni M, Qian ZR, Du J, et al. Tumour micro-environment elicits innate resistance to RAF inhibitors through HGF secretion. Nature 2012;487:500–4.
18. Wilson TR, Fridlyand J, Yan Y, Penuel E, Burton L, Chan E, et al. Widespread potential for growth-factor–driven resistance to anticancer kinase inhibitors. Nature 2012;487:505–9.
19. Barretina J, Caponigro G, Stransky N, Venkatesan K, Margolin AA, Kim S, et al. The Cancer Cell Line Encyclopedia enables predictive modelling of anticancer drug sensitivity. Nature 2012;483:603–7.
20. Garraway LA, Widlund HR, Rubin MA, Getz G, Berger AJ, Ramaswamy S, et al. Integrative genomic analyses identify MITF as a lineage survival oncogene amplified in malignant melanoma. Nature 2005;436:117–22.
21. Yokoyama S, Woods SL, Boyle GM, Aoude LG, MacGregor S, Zismann V, et al. A novel recurrent mutation in MITF predisposes to familial and sporadic melanoma. Nature 2011;480:99–103.
22. Sakurai H, Chiba H, Miyoshi H, Sugita T, Toriumi W. IkappaB kinases phosphorylate NF-kappaB p65 subunit on serine 536 in the transactivation domain. J Biol Chem 1999;274:30353–6.
23. Enzler T, Sano Y, Choo MK, Cottam HB, Karin M, Tsao H, et al. Cell-selective inhibition of NF-kappaB signaling improves therapeutic index in a melanoma chemotherapy model. Cancer Discov 2011;1:496–507.
24. Aronov AM, Tang Q, Martinez-Botella G, Bemis GW, Cao J, Chen G, et al. Structure-guided design of potent and selective pyrimidylpyrrole inhibitors of extracellular signal-regulated kinase (ERK) using conformational control. J Med Chem 2009;52:6362–8.
25. Morris EJ, Jha S, Restaino CR, Dayananth P, Zhu H, Cooper A, et al. Discovery of a novel ERK inhibitor with activity in models of acquired resistance to BRAF and MEK inhibitors. Cancer Discov 2013;3:742–50.
26. Bittner M, Meltzer P, Chen Y, Jiang Y, Seftor E, Hendrix M, et al. Molecular classification of cutaneous malignant melanoma by gene expression profiling. Nature 2000;406:536–40.
27. Sensi M, Catani M, Castellano G, Nicolini G, Alciato F, Tragni G, et al. Human cutaneous melanomas lacking MITF and melanocyte differentiation antigens express a functional Axl receptor kinase. J Invest Dermatol 2011;131:2448–57.
28. Zhang Z, Lee JC, Lin L, Olivas V, Au V, LaFramboise T, et al. Activation of the AXL kinase causes resistance to EGFR-targeted therapy in lung cancer. Nat Genet 2012;44:852–60.
29. Holland SJ, Pan A, Franci C, Hu Y, Chang B, Li W, et al. R428, a selective small molecule inhibitor of Axl kinase, blocks tumor spread and prolongs survival in models of metastatic breast cancer. Cancer Res 2010;70:1544–54.
30. Yakes FM, Chen J, Tan J, Yamaguchi K, Shi Y, Yu P, et al. Cabozantinib (XL184), a novel MET and VEGFR2 inhibitor, simultaneously suppresses metastasis, angiogenesis, and tumor growth. Mol Cancer Ther 2011;10:2298–308.
31. Liu L, Greger J, Shi H, Liu Y, Greshock J, Annan R, et al. Novel mechanism of lapatinib resistance in HER2-positive breast tumor cells: activation of AXL. Cancer Res 2009;69:6871–8.
32. Miller AJ, Du J, Rowan S, Hershey CL, Widlund HR, Fisher DE. Transcriptional regulation of the melanoma prognostic marker melastatin (TRPM1) by MITF in melanocytes and melanoma. Cancer Res 2004;64:509–16.
33. Gray-Schopfer VC, Karasarides M, Hayward R, Marais R. Tumor necrosis factor-alpha blocks apoptosis in melanoma cells when BRAF signaling is inhibited. Cancer Res 2007;67:122–9.
34. Wood KC, Konieczkowski DJ, Johannessen CM, Boehm JS, Tamayo P, Botvinnik OB, et al. MicroSCALE screening reveals genetic modifiers of therapeutic response in melanoma. Sci Signal 2012;5:rs4.
35. Sequist LV, Waltman BA, Dias-Santagata D, Digumarthy S, Turke AB, Fidias P, et al. Genotypic and histological evolution of lung cancers acquiring resistance to EGFR inhibitors. Sci Transl Med 2011;3:75ra26.
36. Johannessen CM, Johnson LA, Piccioni F, Townes A, Frederick DT, Donahue MK, et al. A melanocyte lineage program confers resistance to MAP kinase pathway inhibition. Nature 2013;504:138–42.
37. Boehm JS, Zhao JJ, Yao J, Kim SY, Firestein R, Dunn IF, et al. Integrative genomic approaches identify IKBKE as a breast cancer oncogene. Cell 2007;129:1065–79.
38. Garnett MJ, Edelman EJ, Heidorn SJ, Greenman CD, Dastur A, Lau KW, et al. Systematic identification of genomic markers of drug sensitivity in cancer cells. Nature 2012;483:570–5.
39. Lin WM, Baker AC, Beroukhim R, Winckler W, Feng W, Marmion JM, et al. Modeling genomic diversity and tumor dependency in malignant melanoma. Cancer Res 2008;68:664–73.
40. Subramanian A, Tamayo P, Mootha VK, Mukherjee S, Ebert BL, Gillette MA, et al. Gene set enrichment analysis: a knowledge-based approach for interpreting genome-wide expression profiles. Proc Natl Acad Sci U S A 2005;102:15545–50.
41. Barbie DA, Tamayo P, Boehm JS, Kim SY, Moody SE, Dunn IF, et al. Systematic RNA interference reveals that oncogenic KRAS-driven cancers require TBK1. Nature 2009;462:108–12.
42. Hinata K, Gervin AM, Jennifer Zhang Y, Khavari PA. Divergent gene regulation and growth effects by NF-kappa B in epithelial and mesenchymal cells of human skin. Oncogene 2003;22:1955–64.
43. Seki E, De Minicis S, Osterreicher CH, Kluwe J, Osawa Y, Brenner DA, et al. TLR4 enhances TGF-beta signaling and hepatic fibrosis. Nat Med 2007;13:1324–32.
44. Tian B, Nowak DE, Jamaluddin M, Wang S, Brasier AR. Identification of direct genomic targets downstream of the nuclear factor-kappaB transcription factor mediating tumor necrosis factor signaling. J Biol Chem 2005;280:17435–48.
45. Liberzon A, Subramanian A, Pinchback R, Thorvaldsdottir H, Tamayo P, Mesirov JP. Molecular signatures database (MSigDB) 3.0. Bioinformatics 2011;27:1739–40.